Light Wave Propagation Model for Indoor Visible Light Communication Systems Employing Small LED Sources

Marwa M. A. Elsaaty [1], Adel Zaghloul [2], and Khalid. F. A. Hussein [3]

[1] Institute of Aviation Engineering and Technology (IAET), Egypt
eng.marwamohamed1991@gmail.com

[2] Zagazig University, Faculty of Engineering, Egypt
adel6730101@yahoo.com

[3] Electronics Research Institute (ERI), Cairo, 11843, Egypt
fkhalid@eri.sci.eg, khalid_elgabaly@yahoo.com

Abstract ─ The aim of the present work is to build a robust and computationally efficient model for the light wave propagation in indoor visible light communication (VLC) systems. It is assumed that a small (point) LED source is used inside a room of relatively small dimensions (room area $\leq 5\text{m} \times 5\text{m}$). The light wave is treated as an electromagnetic wave suffering multiple reflections on the walls of the room. The Geometrical Theory of Diffraction (GTD) is applied for evaluation of the light wave reflection on the rough walls of the room. Also, the present work is concerned with developing a new computational method for the assessment of inter-symbol interference (ISI) encountered in such indoor VLC systems. The signal strength, the power of ISI, and hence, the signal-to-ISI ratio (SISIR) are evaluated over the horizontal plane of the mobile units (at a height of about 1m above the room floor). The effects of the room dimensions and some structural parameters such as the reflectance of the side walls on the SISIR are numerically investigated.

Index Terms ─ Inter-Symbol Interference (ISI), Visible Light Communications (VLC).

I. INTRODUCTION

Most of the currently operational wireless communication systems are employing the radio frequency (RF) and microwave spectra. As a consequence of the rapidly increasing number of mobile communication users, the wireless communications face a serious shortage regarding spectrum allocation. The visible light communication (VLC) systems utilize the unlicensed wide spectrum of the visible light for wireless communications [1-5]. The visible light spectrum is capable of offering much higher transmission rates than those offered by RF and microwave spectra. Moreover, the VLC systems are more immune to electromagnetic interference than the microwave wireless communication systems. Also, the VLC systems have the advantage of using the general lighting sources such as the light-emitting diode (LED) through high-speed on/off switching to transmit data at high rates. Photosensitive components such as photodetectors can be used to receive the signals sent by the lighting sources. Thus, the VLC enables the efficient use of the simple on/off keying (OOK) modulation as a digital intensity modulation technique for high data rate transmission with high noise immunity.

In indoor VLC system, the light source should meet the requirement for room lighting in addition to signal coverage. This requires the installation of LED source with appropriate shape and distribution. For a room of, relatively, small area ($\leq 5\text{m} \times 5\text{m}$) the lighting may be performed by employing a single point LED source mounted at the center of the room ceil; see Fig. 1.

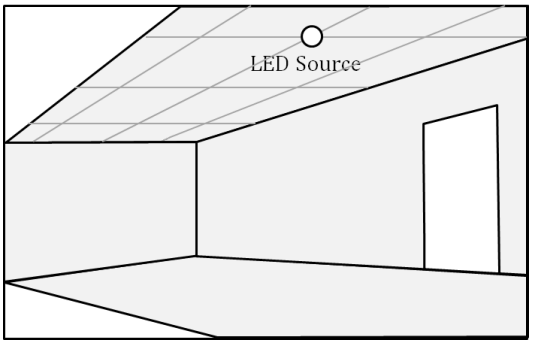

Fig. 1. The VLC system considered in the present work employs a single point LED source for signal coverage inside the room.

In the present study, it is assumed that the responsivity of the photodetector used in the mobile receivers is unity, and its FOV is 90°. The sidewalls of the room are assumed to be Lambertian reflective

Submitted On: April 24, 2021
Accepted On: July 7, 2021

https://doi.org/10.47037/2021.ACES.J.360814

surfaces with unity Lambert index and arbitrary reflectance.

The present work provides a complete description of the method used to evaluate the channel impulse response and inter-symbol interference (ISI) in the plane of the mobile receivers for both types of LED sources. It is shown that when a single point LED source is employed, the ISI results only from the reflection of light on the side walls of the room, i.e., from the non-line-of-sight (non-LOS) propagation.

II. INDOOR VLC CHANNEL MODEL

It is assumed that the room is empty and has its interior of a cuboidal shape whose dimensions are W_x, W_y, and W_z in the x-, y-, and z-directions, respectively. The LED source is assumed to be Lambertian radiator with unity Lambert index and is mounted on the room ceil with the maximum luminous intensity directed normal to the room ceil in the downward direction. On the other hand, the mobile, or even stationary, receivers are assumed as photodetectors that can freely move in the horizontal plane at a height of z_r above the room floor

In the present study, the walls of the room are assumed to be optically rough and, hence, the reflection of the light on these walls depends on the wall reflectance and roughness and can be accurately evaluated using the Geometrical Theory of Diffraction in conjunction with the Ray-Tracing (GTD-RT) method described in [6-8]. For electromagnetic simulation, the room walls are modeled as rough surfaces using the Savitzky-Golay method as described in [9]. The resulting models of the wall surface are found to be Lambertian surfaces with unity Lambert index. As the present study focuses only on the light wave propagation model, the receiving photodetector responsivity is assumed to be unity; $\eta = 1$. Also, the FOV of the receiving photodetector is assumed to be 90°.

Under these conditions, a point in the plane of the receiver units can be illuminated from the following sources:

1. Direct illumination (LOS) from the LED source.
2. Indirect illumination (non-LOS) due to the reflection of the light on the sidewalls of the room.
3. Noise resulting from ambient light of the sun, fluorescent lambs, or any other unplanned source.

A. Impulse response for point light source

It is assumed that a small LED source is used for VLC in the room as shown in Fig. 1. This light source is located at the center of the room ceil as shown in Fig. 2 and can be considered a point source. The luminous flux intensity $I(\theta)$ due to a point LED source mounted in the room ceil is the direction making angle θ with the normal to the ceil (see Fig. 2) is defined as the luminous flux within the unit solid angle at this direction:

$$I_{\mathrm{a}}(\theta) = \frac{d\Phi(\theta)}{d\Omega}, \tag{1}$$

where $d\Phi(\theta)$ is the luminous flux within the solid angle $d\Omega$ in the direction θ.

The radiation from this LED source can be described by the spatial angular distribution of the luminous flux intensity $I_a(\theta)$, which is assumed to be Lambertian with unity Lambert index:

$$I_{\mathrm{a}}(\theta) = I_{\mathrm{a}_0} \cos\theta, \tag{2}$$

where I_{a_0} is maximum luminous flux intensity (in the direction $\theta = 0$ i.e. normal to the room ceiling).

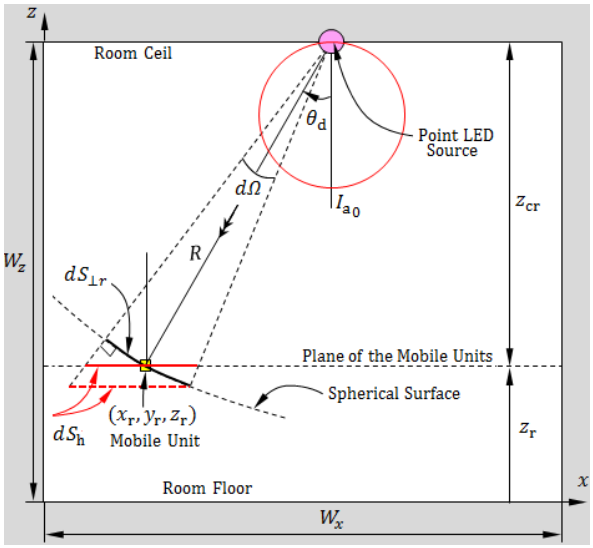

Fig. 2. Light wave propagation model for calculation of the direct (LOS) horizontal illuminance at the location of the mobile unit.

A.1. Direct (LOS) illuminance

The illuminance of a surface segment $\mathrm{dS}_{\perp \mathrm{r}}$ at the location of a receiver at $\mathrm{r_r} \equiv (\mathrm{x_r}, \mathrm{y_r}, \mathrm{z_r})$, (shown in Fig. 2) of a sphere whose center is at the point LED source can be expressed as follows:

$$E_{S_{\perp r}} = \frac{d\Phi}{dS_{\perp \mathrm{r}}} = \frac{I_{\mathrm{a}}(\theta_d)d\Omega}{dS_{\perp \mathrm{r}}}, \tag{3}$$

where $d\Omega$ is the solid angle subtending the area $dS_{\perp \mathrm{r}}$ that is given as:

$$dS_{\perp \mathrm{r}} = R^2 d\Omega, \tag{4}$$

where R is the distance between the LED source and the mobile receiver.

By substitution from (4) into (3), one gets the following expression:

$$E_{S_{\perp r}} = \frac{I_{\mathrm{a}}(\theta_d)}{R^2} = \frac{I_{\mathrm{a}_0} \cos\theta_d}{R^2}. \tag{5}$$

The illuminance of the horizontal surface at $\mathbf{r}_\mathrm{r}$ can be expressed as follows:

$$E_\mathrm{d} = E_{S_{\perp r}} \cos\theta_\mathrm{d} = \frac{I_{\mathrm{a}_0} \cos^2\theta_\mathrm{d}}{R^2}. \tag{6}$$

The distance, R, between the LED source and the mobile receiver can be expressed in terms of the ceil height, z_cr, relative to the plane of the mobile receivers as follows:

$$R = |\mathbf{r}_\mathrm{r} - \mathbf{r}_\mathrm{c}| = \frac{z_\mathrm{cr}}{\cos\theta_\mathrm{d}}, \tag{7}$$

where $\mathbf{r}_\mathrm{c} = (W_x/2, W_y/2, W_z)$ is the position vector of the center point of the room ceil.

The substitution from (7) into (6) results in the following expression for the horizontal illuminance in the plane of the mobile receivers:

$$E_\mathrm{d} \equiv E(\theta_\mathrm{d}) = \frac{I_{\mathrm{a}_0} \cos^4\theta_\mathrm{d}}{z_\mathrm{cr}^2}. \tag{8}$$

The total luminous flux is equal to the total light power, P_{Tx}, radiated from the from the LED source. Hence,

$$P_{Tx} = \int_{\text{half space}} d\Phi = \int_{\text{half space}} I_\mathrm{a}(\theta)\, d\Omega. \tag{9}$$

Considering that $d\Omega = \sin\theta\, d\theta\, d\phi$, the last integral can be expressed as follows:

$$P_{Tx} = \int_0^{2\pi} \int_0^{\pi/2} I_{\mathrm{a}_0} \cos\theta\ \sin\theta\, d\theta\ d\phi. \tag{10}$$

Thus,

$$P_{Tx} = I_{\mathrm{a}_0} \int_0^{2\pi} d\phi \int_0^{\pi/2} \tfrac{1}{2}\sin(2\theta) d\theta. \tag{11}$$

Thus, the maximum luminous flux intensity, I_{a_0}, of the LED source can be expressed in terms of the transmitted optical power, P_{Tx}, as follows:

$$I_{\mathrm{a}_0} = \frac{P_{Tx}}{\pi}. \tag{12}$$

The impulse response due to a point LED source can be expressed as follows:

$$h_\mathrm{d}(t) = \frac{P_{Tx} \cos^4\theta_\mathrm{d}}{\pi z_\mathrm{cr}^2}\ \delta(t - t_\mathrm{a}), \tag{13}$$

where t_a is the time taken by an optical impulse to travel from the LED source at $\mathbf{r}_\mathrm{c}$ to the receiver at $\mathbf{r}_\mathrm{r}$:

$$t_\mathrm{a} = \frac{1}{c_0}|\mathbf{r}_\mathrm{r} - \mathbf{r}_\mathrm{c}| = \frac{z_\mathrm{cr}}{c_0 \cos\theta_\mathrm{d}}, \tag{14}$$

where c_0 is the speed of light in free space.

A.2. Indirect (non-LOS) illuminance

Referring to Fig. 3, the illuminance of the side wall $x = 0$, at a point $\mathbf{r}_\mathrm{w} \equiv (0, y_\mathrm{w}, z_\mathrm{w})$ can be given as,

$$[E_\mathrm{w}]_{\mathbf{r}_\mathrm{w}} = \left[\frac{I_\mathrm{a}(\theta_\mathrm{a})}{R_\mathrm{wa}^2} \cos\theta_\mathrm{wa}\right]_{\mathbf{r}_\mathrm{w}} = I_{\mathrm{a}_0}\left[\frac{\cos\theta_\mathrm{a} \cos\theta_\mathrm{wa}}{R_\mathrm{wa}^2}\right]_{\mathbf{r}_\mathrm{w}}. \tag{15}$$

The power (luminous flux) of the light emitted from the wall segment $dy_\mathrm{w}\, dz_\mathrm{w}$ at the point $\mathbf{r}_\mathrm{w}$ can be expressed as follows.

$$[\Phi_\mathrm{w}]_{\mathbf{r}_\mathrm{w}} = [G_\mathrm{w}\, E_\mathrm{w}]_{\mathbf{r}_\mathrm{w}}\, dx_\mathrm{w}\, dz_\mathrm{w}, \tag{16}$$

where G_w is the wall reflectance at the point $\mathbf{r}_\mathrm{w}$.

The wall segment $dy_\mathrm{w}\, dz_\mathrm{w}$ at the point $\mathbf{r}_\mathrm{w}$ can be considered as a secondary radiator. As the wall is assumed as a Lambertian rough surface, the luminous flux intensity of the light emitted from this wall segment can be expressed as follows:

$$[I_\mathrm{w}(\theta_\mathrm{w})]_{\mathbf{r}_\mathrm{w}} = \left[I_{\mathrm{w}_0} \cos\theta_\mathrm{w}\right]_{\mathbf{r}_\mathrm{w}}, \tag{17}$$

where $\left[I_{\mathrm{w}_0}\right]_{\mathbf{r}_\mathrm{w}}$ is the luminous flux intensity in the direction normal to the wall due to the emission from the wall segment $dy_\mathrm{w}\, dz_\mathrm{w}$ at the point $\mathbf{r}_\mathrm{w}$.

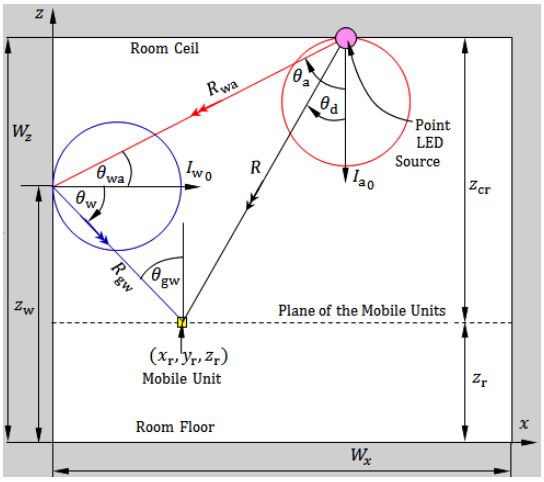

Fig. 3. Light wave propagation model for calculation of indirect (non-LOS) horizontal illuminance at the location of the mobile unit.

Also, the luminance intensity of the light reflected from the wall segment $dy_\mathrm{w}\, dz_\mathrm{w}$ in the direction of the mobile unit at $\mathbf{r}_\mathrm{r}$ can be expressed as follows:

$$[I_\mathrm{w}(\theta_\mathrm{w})]_{\mathbf{r}_\mathrm{w}} = \left[\frac{d\Phi_\mathrm{w}}{d\Omega}\right]_{\mathbf{r}_\mathrm{w}}. \tag{18}$$

Thus, the total luminous flux Φ_w emitted from the wall segment $dy_\mathrm{w}\, dz_\mathrm{w}$ at $\mathbf{r}_\mathrm{w}$ can be obtained as follows:

$$[\Phi_\mathrm{w}]_{\mathbf{r}_\mathrm{w}} = \int_{\text{half space}} [I_\mathrm{w}(\theta)]_{\mathbf{r}_\mathrm{w}}\, d\Omega. \tag{19}$$

Considering that $d\Omega = \sin\theta\, d\theta\, d\phi$, the last integral can be expressed as follows:

$$[\Phi_{\mathrm{w}}]_{\mathbf{r}_{\mathrm{w}}} = \int_0^{2\pi}\int_0^{\pi/2} \left[I_{\mathrm{w}0}\right]_{\mathbf{r}_{\mathrm{w}}} \cos\theta \sin\theta\, d\theta\; d\phi. \quad (20)$$

Thus,

$$[\Phi_{\mathrm{w}}]_{\mathbf{r}_{\mathrm{w}}} = \left[I_{\mathrm{w}0}\right]_{\mathbf{r}_{\mathrm{w}}} \int_0^{2\pi} d\phi \int_0^{\pi/2} \tfrac{1}{2}\sin(2\theta) d\theta. \quad (21)$$

Thus, the total luminous flux $[\Phi_{\mathrm{w}}]_{\mathbf{r}_{\mathrm{w}}}$ emitted from the wall segment $dy_{\mathrm{w}}\, dz_{\mathrm{w}}$ at the point $\mathbf{r}_{\mathrm{w}}$ can be expressed in terms of the maximum luminous flux intensity, $\left[I_{\mathrm{w}0}\right]_{\mathbf{r}_{\mathrm{w}}}$, as follows:

$$[\Phi_{\mathrm{w}}]_{\mathbf{r}_{\mathrm{w}}} = \pi\left[I_{\mathrm{w}0}\right]_{\mathbf{r}_{\mathrm{w}}}. \quad (22)$$

Making use of (15), (16), and (22), the maximum luminous flux intensity, $\left[I_{\mathrm{w}0}\right]_{\mathbf{r}_{\mathrm{w}}}$, can be expressed as follows:

$$\left[I_{\mathrm{w}0}\right]_{\mathbf{r}_{\mathrm{w}}} = \frac{I_{\mathrm{a}0}}{\pi}\left[G_{\mathrm{w}} \frac{\cos\theta_{\mathrm{a}} \cos\theta_{\mathrm{wa}}}{R_{\mathrm{wa}}^2}\right]_{\mathbf{r}_{\mathrm{w}}} dx_{\mathrm{w}}\, dz_{\mathrm{w}}. \quad (23)$$

The horizontal illuminance at the photodetector of the mobile receiver due to the indirect radiation from the wall segment $dy_{\mathrm{w}}\, dz_{\mathrm{w}}$ at $\mathbf{r}_{\mathrm{w}}$ can be expressed as follows:

$$[dE_{\mathrm{i}}]_{\mathbf{r}_{\mathrm{w}}} = \left[\frac{I_{\mathrm{w}0} \cos\theta_{\mathrm{w}}\; \cos\theta_{\mathrm{gw}}}{R_{\mathrm{gw}}^2}\right]_{\mathbf{r}_{\mathrm{w}}}. \quad (24)$$

By substitution from (23) into (24), the following expression is obtained:

$$[dE_{\mathrm{i}}]_{\mathbf{r}_{\mathrm{w}}} = [\xi_i]_{\mathbf{r}_{\mathrm{w}}}\, dxdz, \quad (25)$$

where,

$$[\xi_i]_{\mathbf{r}_{\mathrm{w}}} = \frac{P_{Tx}}{\pi^2}\left[\frac{G_{\mathrm{w}} \cos\theta_{\mathrm{a}} \cos\theta_{\mathrm{wa}} \cos\theta_{\mathrm{w}}\; \cos\theta_{\mathrm{gw}}}{R_{\mathrm{wa}}^2\, R_{\mathrm{gw}}^2}\right]_{\mathbf{r}_{\mathrm{w}}}. \quad (26)$$

Let the indices 1, 2, 3, and 4 be assigned to the walls $x = 0$, $y = 0$, $x = W_x$, and $y = W_y$, respectively. The component of the non-LOS impulse response due to the reflection of light on the wall #1 ($x = 0$) can be expressed as follows:

$$[h_i(\mathrm{t})]_1 = \int_{z_{\mathrm{r}}}^{W_z}\int_0^{W_y} [\xi_i]_{\mathbf{r}_{\mathrm{w}}}\, \delta(t - t_{\mathrm{w}})\, dy_{\mathrm{w}}\; dz_{\mathrm{w}}, \quad (27)$$

where t_{w} is the total time taken by an optical impulse when it is transmitted by the point LED source, then reflected on the surface segment at $\mathbf{r}_{\mathrm{w}}$ (on the wall $x = 0$) and, finally, arrives at the location of the receiver $\mathbf{r}_{\mathrm{r}}$:

$$t_{\mathrm{w}} = \frac{1}{c_0}\left(|\mathbf{r}_{\mathrm{w}} - \mathbf{r}_{\mathrm{c}}| + |\mathbf{r}_{\mathrm{r}} - \mathbf{r}_{\mathrm{w}}|\right). \quad (28)$$

The total non-LOS impulse response at the mobile receiver can be obtained by performing the integration expressed in (27) on each of the four side walls of the room and then summing the integral values as follows:

$$h_i(\mathrm{t}) = \sum_{q=1}^{4} [h_i(\mathrm{t})]_q. \quad (29)$$

Considering that the mobile receiver has its FOV $\leq 90°$, the area of the side wall #1($x = 0$) subtended between the planes $z = z_r$ and $z = W_z$ can be discretized with fine enough resolution to a number of rectangular segments of equal area $\Delta s = \Delta y \Delta z$. The illuminance at the location of the receiver due to the light reflected from the wall segment number m, n can be expressed as follows:

$$\left[\Delta E_{\mathrm{i}_{m,n}}\right]_1 = \left[\Delta s \xi_{i_{m,n}}\right]_1, \quad m = 1,2,..,M_1, \quad n = 1,2,..,N_1 \quad (30)$$

where M_1 and N_1 are the number of segments which the side wall #1 is discretized in the vertical and horizontal directions, respectively, and $\xi_{i_{m,n}}$ is given as follows:

$$\left[\xi_{i_{m,n}}\right]_1 = [\xi_i]_{\mathbf{r}_{\mathrm{w}}=[0,(m-1)\Delta y,(n-1)\Delta z]}. \quad (31)$$

The total (indirect) impulse response due to the light reflection on the four side walls is the horizontal illuminance due to the light arriving at the receiver location through non-LOS propagation and can be expressed as follows:

$$h_{\mathrm{i}}(t) = \sum_{q=1}^{4}\sum_{m=1}^{M_q}\sum_{n=1}^{N_q}\left[\Delta E_{\mathrm{i}_{m,n}}\right]_q \delta\left(t - t_{q,m,n}\right), \quad (32)$$

where M_q and N_q are the number of segments to which the q^{th} side wall is discretized in the vertical and horizontal directions, respectively; $t_{q,m,n}$ is the total time taken by an optical impulse when it is transmitted by the point LED source at $t = 0$, then reflected on the surface segment number m, n on the q^{th} side wall, and finally arrives at the location of the receiver $\mathbf{r}_{\mathrm{r}}$:

$$t_{q,m,n} = \frac{1}{c_0}\left[R_{\mathrm{wa}} + R_{\mathrm{gw}}\right]_{q,m,n}. \quad (33)$$

It is assumed that the OOK modulation technique is employed in the indoor VLC system where the transmitted pulse can be considered as a rectangular pulse of duration equal to the bit period, $T_b = 1/R_b$.

The impulse response due to a point LED source on the ceiling of a cuboidal room can be expressed as the sum of the LOS and non-LOS impulse responses as follows:

$$h(t) = h_{\mathrm{d}}(t) + h_{\mathrm{i}}(t). \quad (34)$$

Upon the knowledge of the total impulse response, $h(t)$, the received pulse can be expressed as follows:

$$s_r(t) = \eta\, s_t(t) \otimes h(t), \quad (35)$$

where η is the responsivity of the receiving photodetector. In the present study, the photodetector responsivity is assumed to be unity; $\eta = 1$.

B. Impulse response due to light source of arbitrary shape

The impulse response due to a point LED source is expressed in (34). A practical LED source that can be commercially available for room lightening may take arbitrary shape extending of a larger area than that of a point LED source. The radiating surface of such a LED source can be planar or three-dimensional. Let the impulse response of an arbitrarily-shaped LED source be designated as $h_{\mathrm{a}}(t)$. For such a LED source, the impulse response can be obtained by integrating $h(t)$ over the surface of the LED source:

$$h_{\mathrm{a}}(t) = \iint_S h(t)\, ds, \tag{36}$$

where S is surface of the LED source that can be of arbitrary shape. The numerical evaluation of (36) requires the discretization (segmentation) of the source surface with enough resolution. Each of the discrete surface elements resulting from the segmentation of LED source surface can be considered as point LED source whose impulse response can be obtained by (34). During the evaluation of the integral in (36) one should take care that the time of arrival parameters t_{a} appearing in (13) and $t_{q,m,n}$ appearing in (32) should be calculated for each discrete surface segment on the LED source surface.

C. Assessment of root-mean-squared propagation delay

In indoor VLC systems, the received optical pulse is subjected to delay spread due to multipath propagation. The transmitted optical pulse representing a bit in the OOK modulation system travels in different paths with variable lengths and, hence, arrives at the position of the receiver at varying times, which causes the received pulse representing a bit to be spread and overlapped with the subsequent bits. The RMS delay spread is a measure of the ISI caused by multipath channel of the indoor propagation.

The average propagation delay, T_{av}, can be calculated once the impulse response $h(t)$ is obtained using the following integral:

$$T_{\mathrm{av}} = \frac{\int_{-\infty}^{\infty} t\, h^2(t)\, dt}{\int_{-\infty}^{\infty} h^2(t)\, dt}. \tag{37}$$

The RMS propagation delay, T_{rms}, can be evaluated as follows:

$$T_{\mathrm{rms}} = \frac{\int_{-\infty}^{\infty} (t - T_{\mathrm{av}})^2\, h^2(t)\, dt}{\int_{-\infty}^{\infty} h^2(t)\, dt}. \tag{38}$$

The integrals (37) and (38) can be numerically evaluated once the impulse response $h(t)$ is determined.

D. Efficient computational method for assessment of power of intersymbol interference and SISIR

The SISIR is the ratio between the light energy of the received pulse to the energy interfering the other pulses due to the delay spread of the received pulse. Thus, the SISIR can be expressed as follows:

$$\mathrm{SISIR} = \frac{E_S}{E_{ISI}} = \frac{\int_{t_{\mathrm{a}}}^{t_{\mathrm{a}}+T_{\mathrm{b}}} s_r(t)\, dt}{\int_{t_{\mathrm{a}}+T_{\mathrm{b}}}^{\infty} s_r(t)\, dt}, \tag{39}$$

where t_a is the time of arrival of the received pulse. The assessment of the SISIR only can be evaluated by numerical evaluation of the integrals in (39).

D.1. Computational procedure for time-domain ray-tracing

In this section, a novel time-domain ray-tracing procedure is described for the calculation of E_S and E_{ISI} appearing in (37). The model developed in the proposed work is based on the GTD-RT method for the assessment of light reflections on the room walls. This method has been computationally applied and experimentally verified in [7] and [8].

The proposed ray-tracing method accounts for the light reflection on the four side walls. It is considered that the LED source is mounted on the room ceiling and the light propagates in the downward directions to illuminate the room and, hence, light reflection on the ceiling surface is neglected. On the other hand, the room floor is assumed to be covered with textures like carpets that are commonly light-absorptive and, hence, the reflections from the room floor are very weak and can be negligible.

According to the theoretical and experimental studies achieved in [7] and [8] (see the reference list of the manuscript), the light reflected from the wall due to second- and higher-order bounces can be negligible when compared to that reflected due to the first-order bounce. Consequently, a first-order ray-tracing technique is applied as it is enough to get accurate assessment of the impulse response and ISI in a closed room.

The following is a concise list of the steps of the proposed procedure for the application of the proposed time-domain ray-tracing method.

1. The area of each of the four sidewalls of the room is divided into a number of square segments with equal area ΔS_W that is small enough to get high resolution.
2. The time is discretized to small divisions Δt with enough resolution. The time origin is that time at which the rays start emitting from the point LED source.
3. Originating at the location of the point LED source, the range of the solid angle $\Omega = 2\pi$ covering the room space (the lower half-space: $0 < \theta < \pi$ and

$0 < \phi < 2\pi$) is equally divided into equal solid angle divisions each $d\Omega$.

4. The light emitted from the point LED source in the direction θ_d is represented by a number of rays within the solid angle division $d\Omega$ around the direction θ_d. The number of rays is proportional to the luminous flux intensity in the direction θ_d.
5. The power associated with each ray δP is equal to luminous flux within the solid angle division $d\Omega$ divided by the number of rays.
6. Each ray starts traveling from the position of the point LED source with the speed of light and is traced alone.
7. If the ray arrives at the location of the mobile receiver without hitting any of the side walls its associated power is added to the direct signal power (LOS path).
8. If the ray hits the same surface segment ΔS_W within the same time division Δt on one of the side walls its associated power is added to the power of ISI (non-LOS path) and the location and time at which this ray hits the side wall is stored.
9. The light illuminating each discrete segment ΔS_W of the side wall surface is calculated by summing power associated with each ray hitting this segment within the same time division Δt.
10. The wall segment ΔS_W is considered as a secondary radiator where the emitted light has the luminous flux can be calculated using (16).
11. The steps from 3 through 7 of the procedure listed above are repeated replacing LED source by the secondary radiator represented by the side wall segment ΔS_W.
12. The list of power and time of arrival calculated and stored as described above are now sorted to calculate the time record of both the LOS and the non-LOS light power arriving at the mobile receiver.
13. If multiple point sources are employed in the VLC, the impulse response, $h_d(t)$, due to the LOS propagation is calculated using (13) and the time record obtained in the step 12 above.
14. The impulse response, $h_i(t)$, due to the non-LOS propagation is calculated by numerical integration of the integral in (27) using the time record obtained in the step 12 above.
15. The total impulse response,$h(t)$, is calculated using (34).
16. If an arbitrarily shaped LED source is employed, the integral in (36) is numerically evaluated to get the total impulse response, $h_a(t)$.

III. RESULTS AND DISCUSSIONS

This section is concerned with the presentation and discussion of the numerical results obtained when the proposed computational model proposed in the previous sections for indoor light wave propagation is applied. It should be noted that the sidewalls of the room are assumed to be Lambertian with reflectance $G = 0.5$.

A. ISI at arbitrary point in indoor VLC system

Consider the case of a mobile unit (receiver) at the point $\mathbf{r} = (1\text{m}, 2\text{m}, 1\text{m})$. The present section is concerned with the investigation of the impulse response at the location of the indicated receiver due to a point LED source mounted at the center of the room ceil.

A.1. Impulse response at arbitrary point

The impulse response at the location $\mathbf{r} = (1\text{m}, 2\text{m}, 1\text{m})$ is presented in Fig. 4. The LOS impulse response is a Dirac-delta function $\delta(t - t_a)$, where $t_a = 8.6$ ns, is the time of arrival of the light impulse transmitted by a point LED source at the center of the room ceil. The non-LOS impulse response is shown in Fig. 4 (b). Each of the four peaks of the impulse response is caused by the light reflection on one of the four side walls of the room. The first peak is the highest one and is caused by light impulse reflection on the nearest wall to the receiver ($x = 0$). The fourth peak is the lowest one and is caused by light reflection on the farthest wall ($x = W_x$).

The total impulse response at the location $\mathbf{r} = (1\text{m}, 2\text{m}, 1\text{m})$ due to a point LED source is shown in Fig. 5. As the level of magnitude of the non-LOS response is very low relative to that of the LOS response, log scale is used for the vertical axis to show both responses together. As shown in this figure, the total impulse response has two distinct components; one is a Dirac-delta function, whereas the other component has a duration over the interval $(13 - 30$ ns) of the delay time.

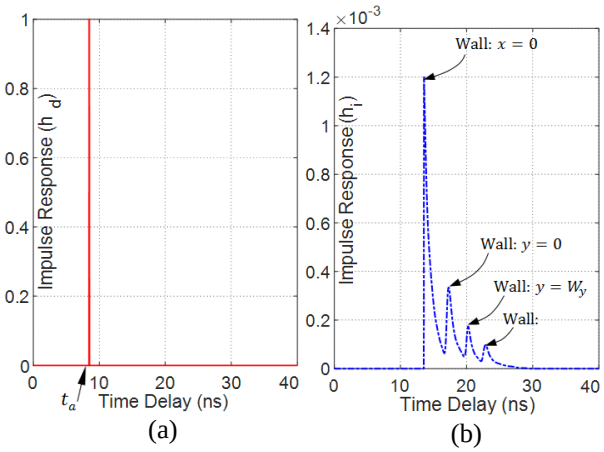

Fig. 4. Normalized impulse response at a point $\mathrm{r} = (1\text{m}, 2\text{m}, 1\text{m})$ inside a room of dimensions $5\text{m} \times 5\text{m} \times 3\text{m}$ due to a point LED source mounted at the center point of the room ceil, (a) LOS impulse response and (b) non-LOS impulse response.

A.2. Received signal at arbitrary point in the horizontal plane

It is assumed that the VLC employs intensity modulation using OOK. Also, it is assumed that the LED source transmits the data at a bit rate $R_b = 50$ Mbps. When a point LED source is used to transmit a pulse that represents a data bit, the pulses that arrive at $\mathbf{r} = (1\text{m}, 2\text{m}, 1\text{m})$ through the LOS and non-LOS are presented in Fig. 6 (a). The total received pulse is presented in Fig. 6 (b) in comparison to the ideal (reference) pulse. The reference pulse is the pulse that would be received if the impulse response were a pure Dirac-delta function, i.e., the pulse received through the LOS from a point LED source. It is shown that the received pulse has two types of distortion; the first type is amplitude distortion due to the addition of the light received through the non-LOS path and the other distortion is caused by the delay-spread due to the delayed light pulse received through the non-LOS path. The power of the ISI is calculated as described in Section II.C resulting in SISIR = 15.75 dB.

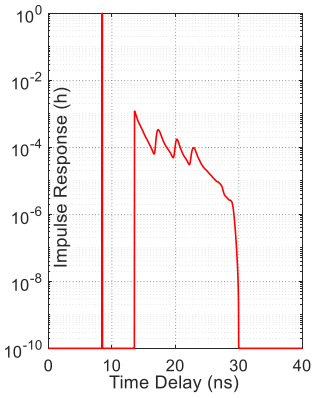

Fig. 5. Total (normalized) impulse response at a point $\mathrm{r} = (1\text{m}, 2\text{m}, 1\text{m})$ inside a room of dimensions $5\text{m} \times 5\text{m} \times 3\text{m}$ due to a point LED source mounted at the center point of the room ceil.

B. ISI at the central point in indoor VLC system

It is assumed that the VLC employs intensity modulation using on-off keying (OOK). Also, it is assumed that the LED source transmits the data at a bit rate $R_b = 50$ Mbps. It transmits a rectangular pulse that represents a data bit. The impulse response, the received pulse, and, hence the ISI are assessed at the center of the horizontal plane of the mobile units ($z = 1\text{m}$).

B.1. Impulse response at the central point in the horizontal plane

Assuming that the mobile unit is at $\mathbf{r} = (2.5\text{m}, 2.5\text{m}, 1\text{m})$, i.e., the center point of the plane $z = z_r$, the impulse response is plotted against the time delay as shown in Fig. 7. For a single LED point source at the center of the room ceil, the LOS impulse response is a Dirac-delta function $\delta(t - t_a)$ as shown in Fig. 10 (a). Thus, the LOS impulse response of a VLC channel employing a point LED source is also an impulse at the time of arrival, t_a, that can be calculated using (14) which gives $t_a = 6.7$ ns. On the other hand, the non-LOS impulse response is spread over the time interval $(8 - 26\text{ ns})$. However, as shown in Fig. 10 (a), the magnitude of the latter is very low relative to that of the former, the latter is very low relative to the former ($\max(h_i) \sim 10^{-4} \max(h_d)$). Thus, for a point LED source, no spread delay is caused by the LOS illuminance; the spread delay and, hence, the ISI are caused only by the non-LOS illuminance which is very small in comparison to the LOS illuminance.

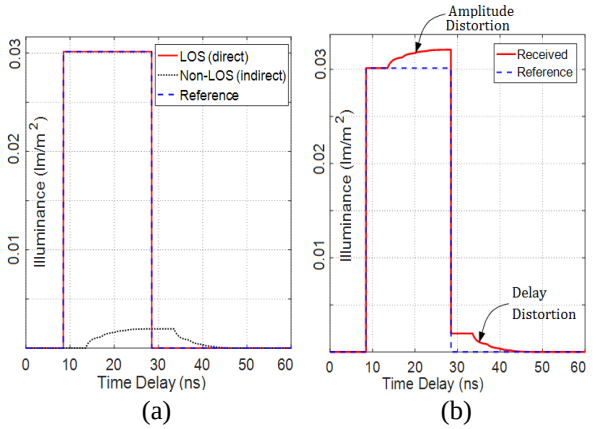

Fig. 6. The received optical pulse due to a single point LED source at the ceil center in indoor VLC at the point $\mathrm{r} = (1\text{m}, 2\text{m}, 1\text{m})$ in a room of dimensions $5\text{m} \times 5\text{m} \times 3\text{m}$. (a) Components of the received pulse: LOS and non-LOS, and (b) total received pulse.

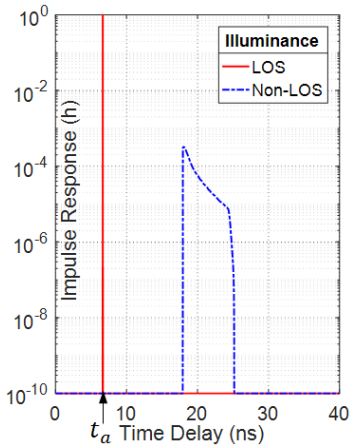

Fig. 7. Normalized impulse response due to direct (LOS) propagation and indirect (non-LOS) propagation in indoor VLC at the point (2.5m, 2.5m, 1.0m) in a room of dimensions $5\text{m} \times 5\text{m} \times 3\text{m}$ when a point LED source is mounted at the ceil center.

B.2. Received signal at the central point in the horizontal plane

When a point LED source is used to transmit a rectangular pulse of duration $T_b = 1/R_b$, the pulse arriving through the LOS and that arriving through the non-LOS at $\mathbf{r}_r = (2.5\text{m}, 2.5\text{m}, 1\text{m})$ are shown in Fig. 8. The total received pulse is shown in Fig. 1 (b) in comparison to the reference pulse. It shown that the received pulse has two types of distortion; the first type is amplitude distortion due to the addition of the light received through the non-LOS path and the other distortion is caused by the delay-spread due to the delayed light pulse received through the non-LOS path. However, the received pulse is weakly distorted and, hence, the resulting SINR is 19.4 dB.

C. Distribution of illumination on the horizontal plane

The distribution of the received signal (without ISI) in the plane of the mobile units ($z = 1\text{m}$) is presented in Fig. 9 inside a room of dimensions $5\text{m} \times 5\text{m} \times 3\text{m}$. The point LED source is mounted on the room ceil at its center point and the mobile receiving photodetectors are assumed to have FOV $= 90°$ and responsivity $\eta = 1$.

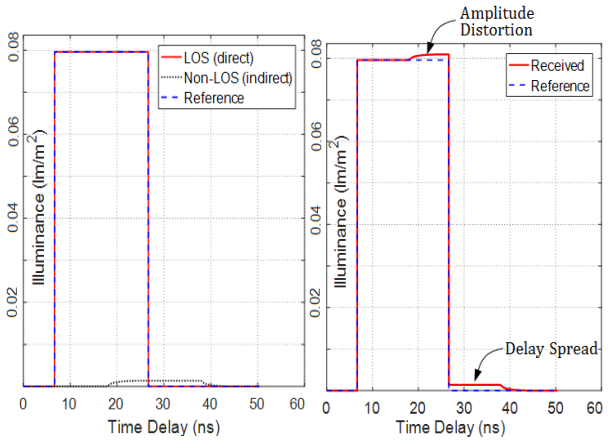

Fig. 8. The received optical pulse due to a single LED point source at the ceil center in indoor VLC at the point $(2.5\text{m}, 2.5\text{m}, 1.0\text{m})$ in a room of dimensions $5\text{m} \times 5\text{m} \times 3\text{m}$. (a) Components of the received pulse: LOS and non-LOS, and (b) total received pulse.

D. Distribution of the SISIR in the horizontal plane

The distribution of the SISIR in the plane of the mobile units ($z = 1\text{m}$) is presented in Fig. 10 for a VLC system employing a point LED source inside a room of dimensions $5\text{m} \times 5\text{m} \times 3\text{m}$. The light source is mounted on the room ceil at its center point and the mobile receiving photodetectors are assumed to have FOV $= 90°$ and responsivity $\eta = 1$. It is clear that the SISIR in the horizontal plane is maximum near the room center and minimum near the room corners.

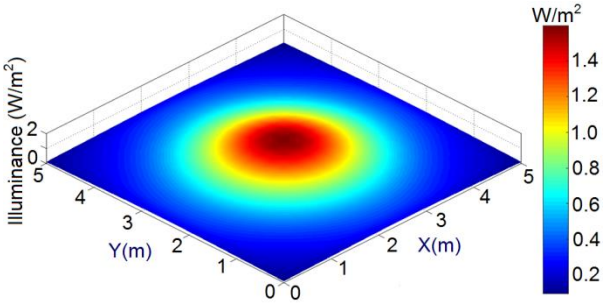

Fig. 9. Distribution of the received signal (without ISI) in the plane of the mobile receivers ($z = 1\text{m}$) in a VLC system inside a room of dimensions $5\text{m} \times 5\text{m} \times 3\text{m}$; a point LED source is mounted on the room ceil at its center point; the mobile receivers have FOV $= 90°$.

E. Effect of the room dimensions structural parameters on the SISIR

The room dimensions and the structural parameters including the optical properties of the wall material, color and suface roughness have significant effects on the perfromance of the indoor VLC system. The dependence of the SISIR on the reflectance of the side walls in a VLC system inside a room of height 3m and different areas is presented in Fig. 11 when the mobile receiver is at the center of the room area and near one of the room corners. As the ISI is mainly caused by the reflections of the side walls of the room, increasing the wall reflectance leads to significant decrease of the SISIR irrespective of the location of the mobile receviver.

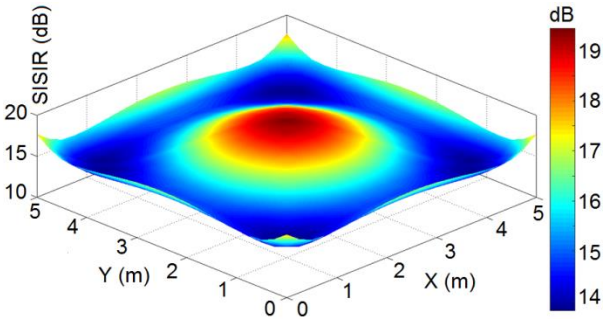

Fig. 10. Distribution of the SISIR in the plane of the mobile units ($z = 1\text{m}$) in VLC system inside a room of dimensions $5\text{m} \times 5\text{m} \times 3\text{m}$; a point LED source is mounted on the room ceil at its center point; the mobile receivers have FOV $= 90°$.

As shown in Fig. 11 (a), increasing the room dimensions has a great effect on the indoor VLC

perfromance and leads to increase the SISIR at the center point of the room because the center point is farther from the side walls when the room is wider. Howerver, increasing the room dimensions has a weak effect on the SISIR in the regions near the room corners. As shown in Fig. 11 (b), the SISIR at the point (0.5m, 0.5m, 1.0m) is slightly decreased due to increasing the room diemnsions because this point is closer to the LED source when the room is smaller.

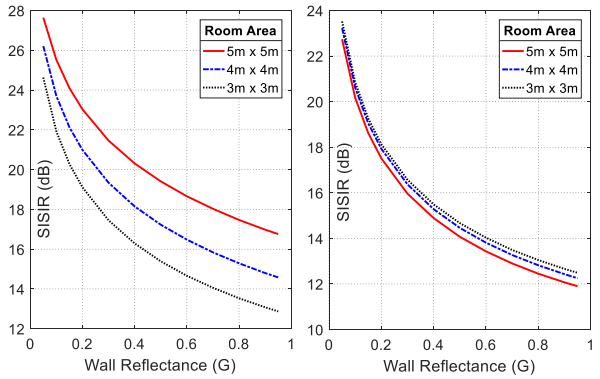

Fig. 11. Dependence of the SISIR on the reflectance of the side walls in VLC system inside a room of height 3m and different areas. The mobile receiver is at (a) the center point of the room area, and (b) the point (0.5m, 0.5m) near the room corner.

IV. CONCLUSION

A robust computational model has been introduced for the light wave propagation in indoor VLC systems employing small LED source inside a room of area $\leq 5\text{m} \times 5\text{m}$. The light wave is treated as an electromagnetic wave suffering multiple reflections on the walls of the room. The GTD-RT technique is applied for evaluation of the light wave reflection of the rough surfaces of the room walls. Moreover, an efficient computational method has been described for the assessment of the ISI encountered in indoor VLC system. The distribution of the SISIR is numerically evaluated over the horizontal plane of the mobile units (at a height of about 1m above the room floor). The effects of the room dimensions and some structural parameters such as the reflectance of the side walls on the SISIR have been investigated numerically. It has been shown that a narrower room has worse effect on the SISIR.

REFERENCES

[1] Y. Chen, S. Li, and H. Liu, "Dynamic frequency reuse based on improved tabu search in multi-user visible light communication networks," *IEEE Access*, vol. 7, pp. 35173-35183, 2019.

[2] I. Abdalla, M. Rahaim, and T. Little, "Interference in multi-user optical wireless communications systems," *Philosophical Transactions of the Royal Society A*, 378.2169, 20190190, 2020.

[3] K. Lee, H. Park, and J. R. Barry, "Indoor channel characteristics for visible light communications," *IEEE Communications Letters*, vol. 15, no. 2, pp. 217-219, 2011.

[4] K. Lee and H. Park, "Channel model and modulation schemes for visible light communications," In *2011 IEEE 54th International Midwest Symposium on Circuits and Systems (MWSCAS)*, pp. 1-4, Aug., 2011.

[5] T. Komine and M. Nakagawa, "Fundamental analysis for visible-light communication system using LED lights," *IEEE Transactions on Consumer Electronics*, vol. 50, no. 1, pp. 100-107, 2004.

[6] H. H. Qamar, K. F. A. Hussein, and M. B. El-Mashade, "Assessment of signal strength in indoor optical wireless communications using diffuse infrared radiation," In *2019 36th National Radio Science Conference (NRSC)*, pp. 108-117, 2019.

[7] H. H. Qamar, A. E. Farahat, K. F. A. Hussein, and M. B. El Mashade, "Assessment of scattering of plane waves on optically illuminated area of rough surface," *Progress In Electromagnetics Research*, vol. 86, pp. 77-102, 2020.

[8] H. H. Qamar, M. B. El-Mashade, A. E. Farahat, and K. F. A Hussein, "Convergence of ensemble averaging for optical scattering on rough surfaces using GTD-RT," In *6th International Conference on Advanced Control Circuits and Systems (ACCS) & 2019 5th International Conference on New Paradigms in Electronics & Information Technology (PEIT), IEEE*, pp. 167-175, 2019.

[9] S. A. M, Soliman, A. E. Farahat, K. F. A. Hussein, and A.E. A. Ammar, "Spatial domain generation of random surface using Savitzky-Golay filter for simulation of electromagnetic polarimetric systems," *Applied Computational Electromagnetics Society Journal*, vol. 34, no. 1, 2019.